INTERFACE BETWEEN EARTHQUAKE GROUND MOTIONS AND STRUCTURAL RESPONSE: NUMERICAL MODELING AND SIMULATION OF ESSI BEHAVIOR

B. JEREMIĆ[1,2], Y. FENG[1], H. YANG[1], H. WANG[1], D. KOVACEVIĆ[1], A. RODGERS[3] D. MCCALLEN[2]

[1]University of California, Davis, California, USA

[2]Lawrence Berkeley National Laboratory, Berkeley, California, USA

[2]Lawrence Livermore National Laboratory, Livermore, California, USA

Abstract. It has been postulated that interaction of dynamics of three components, an earthquake, soil/rock and the structure, controls the response of structures, systems and components (SSCs) in nuclear installations. It has also been postulated that the Earthquake Soil Structure Interaction (ESSI) can sometimes be beneficial and sometimes detrimental to dynamic response of nuclear installations. Presented in this paper is an analysis of nonlinear, inelastic behavior of deeply embedded nuclear installation, a small modular reactor (SMR), subjected to realistic seismic wave field. The main focus is on developing analysis results with low modeling uncertainty, that can then be used to improve safety and economy of nuclear installations. To that end, focus is on seismic wave fields and inelastic material modeling.

Key Words: Earthquake Soil Structure Interaction (ESSI) Modeling and Simulation.

INTRODUCTION

Modeling and simulation (MS) of earthquake soil structure interaction (ESSI) behavior for nuclear installations requires expertise in a number of areas, including seismology, geotechnical and structural engineering, computational sciences, as well as a sound engineering judgement. Accurate modeling and simulation of earthquake soil structure interaction can reveal new knowledge about behavior of soil structure nuclear installation systems. On one side, potentially beneficial behavior can be discovered and taken advantage of in order to improve economy of nuclear installations. On the other side, potentially detrimental behavior can also be discovered, and design and retrofit measures can be implemented to improve safety of nuclear installations.

Deep embedment of some nuclear installation creates a number of modelling challenges. In this paper, emphasis is placed on inelastic material behavior for soil and contact zone, as well as on three dimensional (3D) seismic motions and their effects on seismic response of nuclear installation.

MODELING AND SIMULATION

3D Seismic Motions

Development of free field motions was performed using SW4 program [Sjögreen and Petersson, 2011; Petersson and Sjögreen, 2017]. A magnitude 7.0 scenario earthquake on the Hayward fault in San Francisco Bay Area in Northern California was used to develop seismic motions Rodgers et al. [2018]. The shear wave velocity of soils in surface layer, that is 500m thick, is $V_s = 500$m/s.

The characteristic ground motions recorded at ESSI nodes are plotted in Figure 1. The peak ground acceleration (PGA) in x and y direction is about 1g. Apart from that, significant amount of vertical motions with PGA $0.4g$ is also observed. Vertical motions are results of surface, Rayleigh waves. This is significant in this case as modeling vertical motions as a result of P waves might not be appropriate in this case [Abell et al., 2018]. Fourier transformation and response spectrum of the motions are shown in figure 2. The frequency range of the motion is within 15Hz. The dominant frequency of the motion is around 5 Hz.

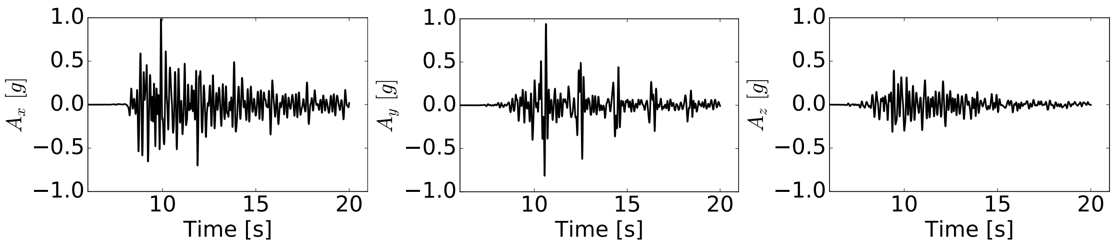

Figure 1: Acceleration and Displacement Time Series of Motion

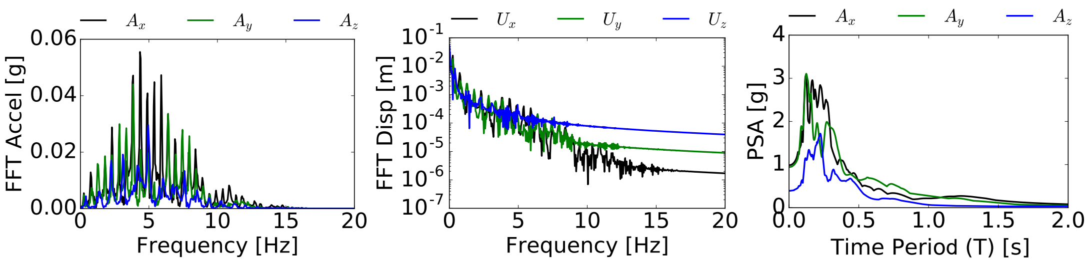

Figure 2: Strong Motion Fourier Transform and Response Spectrum

Seismic Input into Finite Element Model

Input seismic motions into finite element model is done using the Domain Reduction Method (DRM) [Bielak et al., 2003; Yoshimura et al., 2003]. Domain Reduction Method is, to our knowledge, the only method that allows for input of body and surface waves into finite element models. In addition, the DRM resolves the problem of radiation damping analytically for free field models. For the SSI models, the additional wave field, originating from oscillation of SSCs, can be successfully damped out due to their low energy and well defined frequency content.

SMR Model

SMR finite element model is shown in Figure 3.

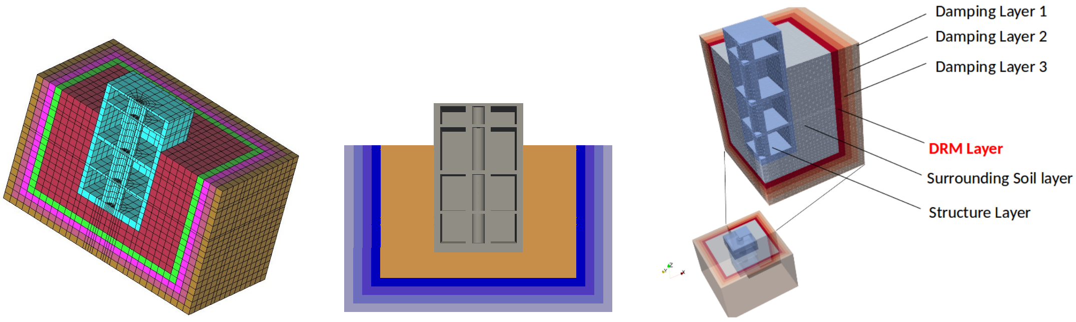

Figure 3: Generic model of deeply embedded small modular reactor (SMR).

The size of the model is 72m×72m×56m. The average mesh size is 3 meters, with 27 node brick elements, that feature quadratic displacement interpolation field. In order to properly propagate seismic waves of different frequencies, mesh size needs to satisfy certain conditions as note by Lysmer and Kuhlemeyer [1969]. When soil plastifies, wave propagation conditions still need to be satisfied, for softer, elastic-plastic material, as noted by Watanabe et al. [2016]. For given finite element mesh with 27 node bricks with average size of 3 meters the minimum wave length properly propagated is 9 meters, using three quadratic elements per wave length. Considering shear wave velocity $v_s = 500m/s$, the maximum frequency for elastic wave propagation is $f_{max} = v_s/\lambda_{min} \leq 56$Hz. For elastic-plastic material, when the stiffness is reduced to half (for example when shear stiffness is reduced to $G/G_{max} = 0.50$), the model is capable of propagating frequencies of up to $f_{max} \leq 14$Hz.

Soil and Contact Model

The soil is assumed to be a saturated backfill with undrained behavior with shear velocity of $V_s = 500$m/s, unit weight of $\rho = 21.4$kPa and Poisson's ratio of $\nu = 0.25$. Full saturation requires limited or no volume change for soil. In this case, von Mises type material model and total stress analysis is used [Pecker et al., 2018]. This ensures that plastic strain, that form largest portion of total strain, do not have a volumetric component. Hence use of Poisson's ratio of $\nu = 0.25$ for elastic portion of strain response creates minor total volumetric strain, which is consistent with the actual behavior of saturated soil behavior. Soil undrained shear strength S_u is determined to be $S_u = 650kPa$ based on empirical correlation to the shear wave velocity $V_s[m/s] = 23(S_u[kPa])^{0.475}$ [Dickenson, 1994]. It is highly recommended to perform tests on actual soil at the site in order to obtain material parameters. Using empirical correlations, as the one above, introduces significant uncertainty in material parameters, and this uncertainty can be reduced by performing site specific material testing [Phoon and Kulhawy, 1999a,b].

Node-to-node penalty soft contact element is used to model the interaction between foundation and soil [Sinha and Jeremić, 2017]. Soft contact constitutive model accounts for gradual increase in contact force between concrete and the soil for compressive behavior and a possibility of gap opening for tensile behavior. Soft contact model also accounts for nonlinear shear slip. For this model, a nonlinear shear slip is assumed with low friction angle of $\phi = 14^o$. Such low friction angle is found in contacts of formed concrete with different types of soil [NAVFAC, 1986]. It is again recommended to perform test on site specific soil and concrete material, however values from published results can be used as a first data point for a sensitivity studies, that can be used to investigate in more detail a need for detailed testing of certain properties.

Figure 4 shows soil elastic plastic shear response as well as stiffness curve for the contact model.

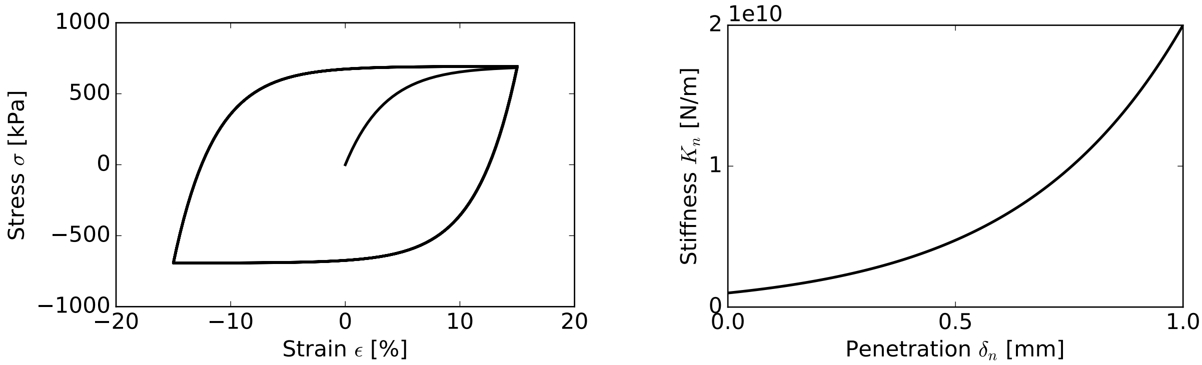

Figure 4: Left: Soil shear stress – shear strain response; Right: Concrete foundation – soil contact axial response.

Staged Simulation

Nonlinear simulation process applies loads in loading stages, each load in a stage is then applied in load increments, that are then iterated toward equilibrium [Felippa, 1993], as shown in Figure 5. Presented analysis uses two loading stages. First stage is a static self-weight load that is used to initialize stress state for the soil, contact elements and the structure. In second stage, seismic motion was applied using DRM method. For each stage, equilibrium is achieved us-

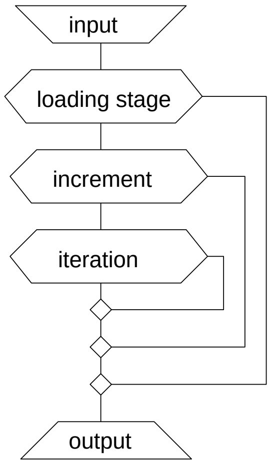

Figure 5: Inelastic, nonlinear analysis cycles, consisting of loading stages, load increments and equilibrium iterations.

ing full Newton-Raphson method with a small tolerance of $TOL = 10^{-4}$N on second-norm of unbalanced force [Crisfield, 1991, 1997]. For dynamic analysis, Newmark integration method with numerical damping ($\gamma = 0.7$) is used [Argyris and Mlejnek, 1991; Hughes, 1987]. Viscous, Rayleigh damping of 2% for structure and 30% for saturated soil is used as well.

All the analysis was performed on Amazon Web Services (AWS) parallel computers in the computing cloud (mostly on AWS computers in Oregon, Idaho and Ireland), using the parallel version of MS ESSI (Real ESSI) Simulator (`http://ms-essi.info/`), [Jeremić et al., 2018]. Cost of multiple analysis cases, charged by the AWS, was on the order of few dozen US dollars.

Inelastic Effects: Results

Free field accelerations, for elastic and inelastic cases, as they change with depth, are shown in Figure 6. It is noted that even for the free field, inelastic response of soil does reduce motions.

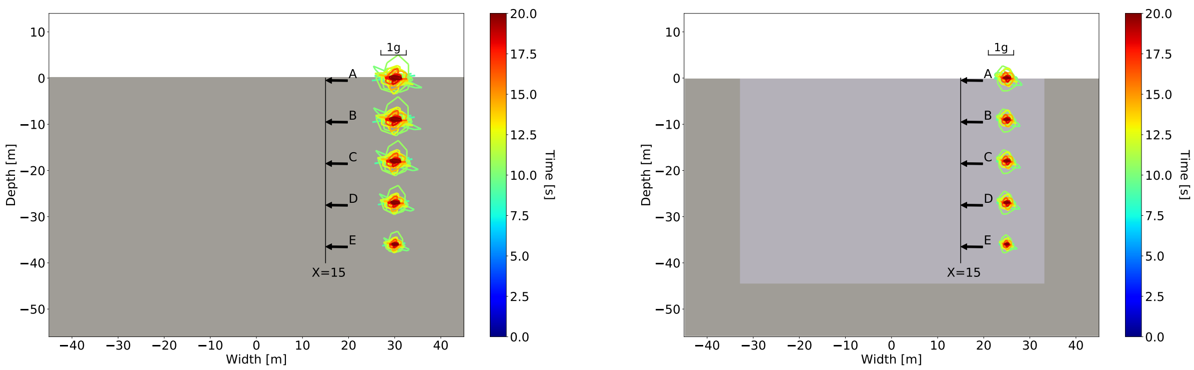

Figure 6: Free field response, left: elastic, right, inelastic.

Figure 7 shows time series of acceleration response at the top center of SMR for ESSI analysis. Significant acceleration decreases is observed for the inelastic case. The acceleration difference in vertical direction is less significant than in horizontal direction.

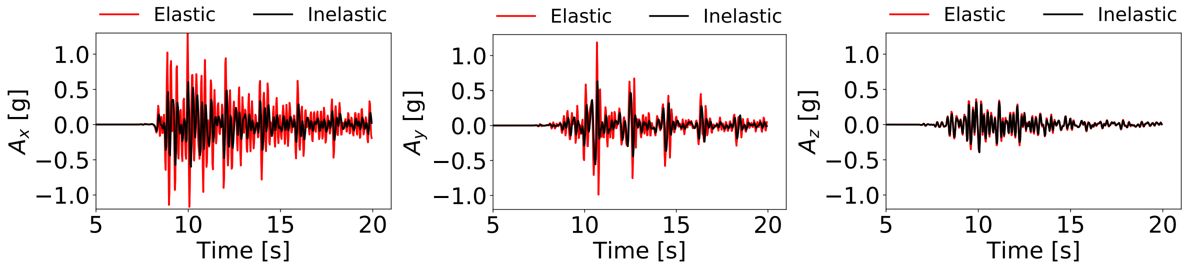

Figure 7: Time series of acceleration response at top center of SMR model.

Figure 8 shows Fourier magnitude of response at the top center of SMR model. It is noted that high frequency component of horizontal acceleration was significant decreased in inelastic case.

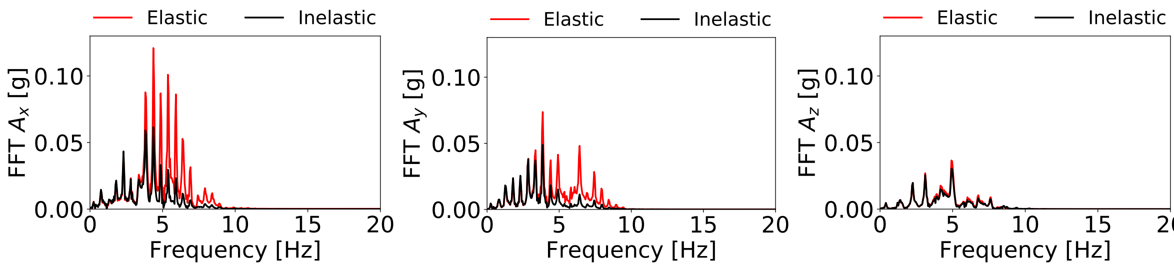

Figure 8: Acceleration response in frequency domain for top of SMR.

Soil structure interaction seismic motions, for elastic and inelastic cases, as they change with depth, along the edge of the SMR, are shown in Figure 9.

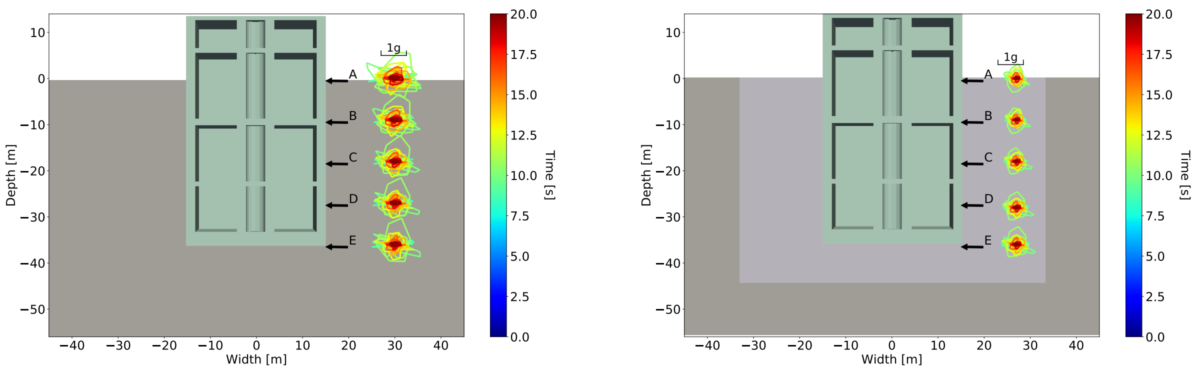

Figure 9: ESSI for an SMR response, left: elastic, right, inelastic.

Figure 10 shows envelope of variations of peak ground accelerations (PGA) and peak ground displacements (PGD) for free field and SSI models. It is noted that PGA and PGD for the SSI

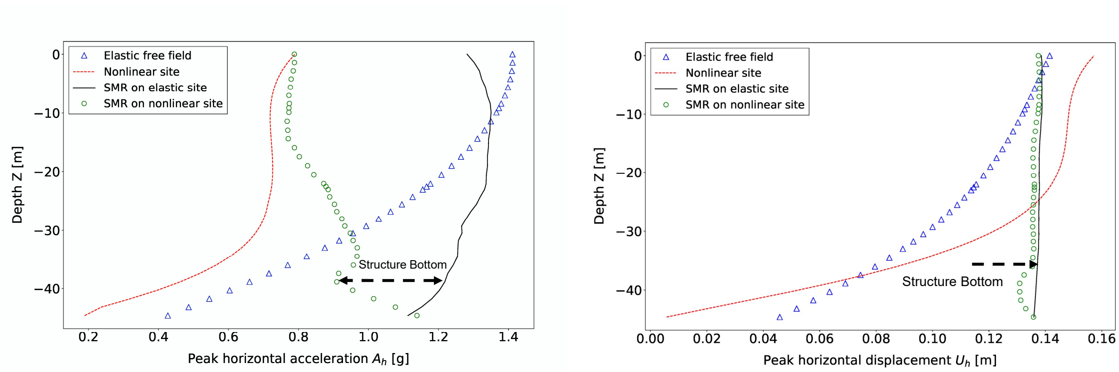

Figure 10: Envelopes of PGA and PGD with depth for linear elastic and inelastic cases, for free field and SSI models.

systems are quite different from free field system, emphasizing again the need to perform full SSI analysis for objects of significant mass, stiffness and embedment. In addition, nonlinearities in soil and contact zone have significant effect on acceleration and displacement response. Accelerations are for the most part reduced, while displacements are, for the most part increased.

In addition to observing acceleration and displacement results for different components of the soil structure system, it is useful to follow energy dissipation in the SSI system. Recently developed energy dissipation framework [Yang et al., 2017] is used to follow incremental and cumulative energy dissipation in SMR model, in time and space. Both inelastic contact an inelastic soil energy dissipation is modeled and followed. Figure 11 shows a snapshot of energy dissipation analysis animation. In addition to energy dissipation, shown are three components of displacements. Actual animation is also available as an MP4 animation movie, by clicking on the figure.

SUMMARY

Presented was modeling and simulation approach for a deeply embedded nuclear installation, a small modular reactor. From a number of challenges associated with modeling such nuclear installation, emphasis in this paper was on fully 3D seismic motions, and on inelastic modeling of soil and the contact zone.

It was shown that inelastic behavior is quite different from linear elastic behavior. Differences in behavior can be beneficial for some aspects of SSI response. For example, acceleration response is usually, but not always, reduced. On the other hand some aspects of SSI response are disadvantaged by inelastic response. For example, displacements tend to increase, usually, but not always, when compared to elastic behavior.

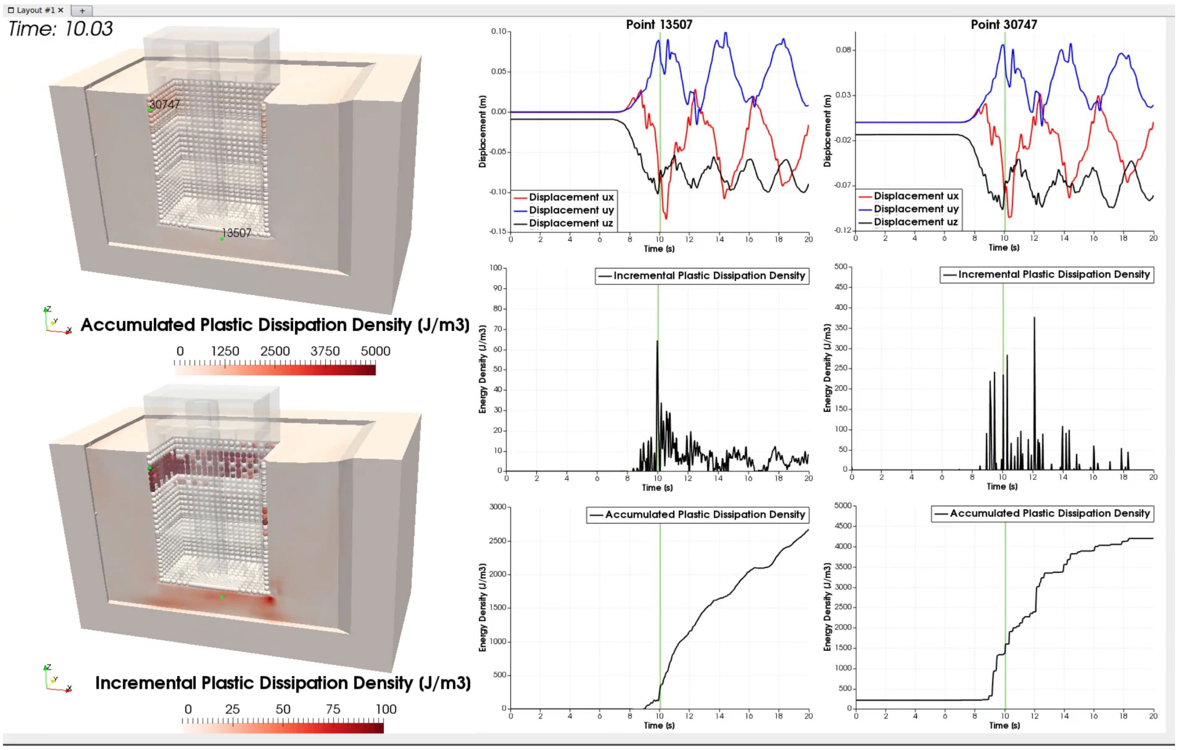

Figure 11: Snapshot of energy dissipation for an SMR. Animation is available online through a live link by clicking on the figure.

Higher fidelity modeling of nuclear installations, taking into account more realistic seismic motions, and more realistic inelastic behavior of materials, can be used to improve safety and economy. Numerical modeling and simulation programs that are capable of performing a wide range of levels of sophistication of modeling are available and can and should be used for design and assessment. One such numerical modeling and simulation program that was used in this study is MS ESSI (Real ESSI) Simulator system (`http://ms-essi.info/`), [Jeremić et al., 2018]. MS ESSI Simulator is available on Amazon Web Services (AWS) computers around the world.

REFERENCES

J. A. Abell, N. Orbović, D. B. McCallen, and B. Jeremić. Earthquake soil structure interaction of nuclear power plants, differences in response to 3-d, 3×1-d, and 1-d excitations. *Earthquake Engineering and Structural Dynamics*, 2018. doi: 10.1002/eqe.3026. URL `https://onlinelibrary.wiley.com/doi/abs/10.1002/eqe.3026`.

J. Argyris and H.-P. Mlejnek. *Dynamics of Structures*. North Holland in USA Elsevier, 1991.

J. Bielak, K. Loukakis, Y. Hisada, and C. Yoshimura. Domain reduction method for three–

dimensional earthquake modeling in localized regions. part I: Theory. *Bulletin of the Seismological Society of America*, 93(2):817–824, 2003.

M. A. Crisfield. *Non–Linear Finite Element Analysis of Solids and Structures Volume 1: Essentials*. John Wiley and Sons, Inc. New York, 605 Third Avenue, New York, NY 10158–0012, USA, 1991.

M. A. Crisfield. *Non–Linear Finite Element Analysis of Solids and Structures Volume 2: Advanced Topics*. John Wiley and Sons, Inc. New York, 605 Third Avenue, New York, NY 10158–0012, USA, 1997.

S. E. Dickenson. *Dynamic response of soft and deep cohesive soils during the Loma Prieta earthquake of October 17, 1989*. PhD thesis, University of California, Berkeley, 1994.

C. A. Felippa. Nonlinear finite element methods. Lecture Notes at CU Boulder, 1993.

T. Hughes. *The Finite Element Method ; Linear Static and Dynamic Finite Element Analysis*. Prentice Hall Inc., 1987.

B. Jeremić, G. Jie, Z. Cheng, N. Tafazzoli, P. Tasiopoulou, F. P. J. A. Abell, K. Watanabe, Y. Feng, S. K. Sinha, F. Behbehani, H. Yang, and H. Wang. *The MS ESSI / Real ESSI Simulator System*. University of California, Davis and Lawrence Berkeley National Laboratory, 2018. `http://ms-essi.info/`.

J. Lysmer and R. L. Kuhlemeyer. Finite dynamic model for infinite media. *Journal of Engineering Mechanics Division, ASCE*, 95(EM4):859–877, 1969.

NAVFAC. *Foundations & Earth Structures, DESIGN MANUAL 7.02*. Naval Facilities Engineering Command, 200 Stovall Street, Alexandria, Virginia 22332-2300, USA, revalidated by change 1 september 1986 edition, 1986.

A. Pecker, J. J. Johnson, and B. Jeremić. *Earthquake Soil Structure Interaction Modeling and Simulation for Nuclear Power Plants*. TECDOC. United Nations (UN), International Atomic Energy Agency (IAEA), Vienna, Austria, 2018.

N. A. Petersson and B. Sjögreen. High order accurate finite difference modeling of seismo-acoustic wave propagation in a moving atmosphere and a heterogeneous earth model coupled across a realistic topography. *Journal of Scientific Computing*, pages 1–34, 2017.

K.-K. Phoon and F. H. Kulhawy. Characterization of geotechnical variability. *Canadian Geotechnical Journal*, 36:612–624, 1999a.

K.-K. Phoon and F. H. Kulhawy. Evaluation of geotechnical property variability. *Canadian Geotechnical Journal*, 36:625–639, 1999b.

A. Rodgers, A. Pitarka, N. Petersson, B. Sjögreen, and D. McCallen. Broadband (0-4 hz) ground motions for a magnitude 7.0 Hayward fault earthquake with 3d structure and topography. *Geophys. Res. Lett.*, 45, 2018. doi: 10.1002/2017GL076505.

S. K. Sinha and B. Jeremić. Modeling of dry and saturated soil-foundation contact. Technical Report UCD–CompGeoMech–01–2017, University of California, Davis, August 2017.

B. Sjögreen and N. A. Petersson. A Fourth Order Accurate Finite Difference Scheme for the Elastic Wave Equation in Second Order Formulation. *J. Sci. Comput.*, 52(1):17–48, 2011. ISSN 0885-7474. doi: 10.1007/s10915-011-9531-1. URL `http://link.springer.com/10.1007/s10915-011-9531-1$\delimiter"026E30F$nhttps://computation-rnd.llnl.gov/serpentine/pubs/wpp4th2011.pdf$\delimiter"026E30F$nhttps://computation-rnd.llnl.gov/serpentine/publications.html`.

K. Watanabe, F. Pisanò, and B. Jeremić. A numerical investigation on discretization effects in seismic wave propagation analyses. *Engineering with Computers*, pages 1–27, 2016. ISSN 1435-5663. doi: 10.1007/s00366-016-0488-4. URL `http://dx.doi.org/10.1007/s00366-016-0488-4`.

H. Yang, F. McKenna, D. B. McCallen, and B. Jeremić. Energy dissipation analysis of elastic-plastic structural elements. *Computer Methods in Applied Mechanics and Engineering, in review*, 2017.

C. Yoshimura, J. Bielak, and Y. Hisada. Domain reduction method for three–dimensional earthquake modeling in localized regions. part II: Verification and examples. *Bulletin of the Seismological Society of America*, 93(2):825–840, 2003.